UDC 621.383.5

AMORPHOUS SILICON SOLAR CELLS

Yoshiyuki Uchida
Hiroshi Sakai
Takeshige Ichimura
Masaharu Nishiura
Hiromu Haruki

I. INTRODUCTION

A photovoltaic power generation has been recognized year by year as one of the most promising candidates for new energy resources.

The key for success in the photovoltaic power generation is a sharp reduction in the price of solar cell. Since the solar energy falling on the ground on a clear day is about 1 kW/m^2, a power generating equipment producing 1 kW maximum needs the solar cell array over 10m^2 if its conversion efficiency is 10%. At present even the solar cell alone in this equipment will cost several million yens because solar cells are so expensive as to be several thousand yens per 1 W.

Hence in the Sunshine Project, the national project for researching the new energy resource as a substitute of petroleum, the price of solar cell is aimed to be reduced to 1/100 of that of 1974. (in the year the research and development started.) Toward the goal, a utilization of silicon ribbon, thin film polycrystalline, compound semiconductor and so on has been studied to obtain economically better solar cells than the conventional single crystal silicon cells and many results have been reported .

In addition to these solar cells, an amorphous silicon solar cell has recently gathered particular attentions. The amorphous silicon is expected to be a low price solar cell material, and in the Sunshine Project an active research and development of amorphous silicon solar cells has been promoted since 1979.

II. THE SUITABILITY OF AMORPHOUS SILICON TO A SOLAR CELL

Recently amorphous materials have been noticed not only in the field of semiconductors but also in the fields of metal, dielectric and magnetic materials. The term "amorphous" generally denotes an amorphous solid which is non-crystalline.

Figure 1 (b) shows a structural model of the amorphous silicon[1] (hereinafter written as to a-Si). Silicon atoms are bonded with neighboring atoms in a covalent bond with a regular configuration in a single crystal silicon [*Fig. 1* (a)], while in the a-Si the configuration is irregular. Therefore, the a-Si considerably differs from the single crystal silicon not only in its electrical and optical properties but in production techniques.

The a-Si is a material suitable to low cost solar cells and has gathered attention by the following reasons:

(a) The energy required in manufacturing the a-Si

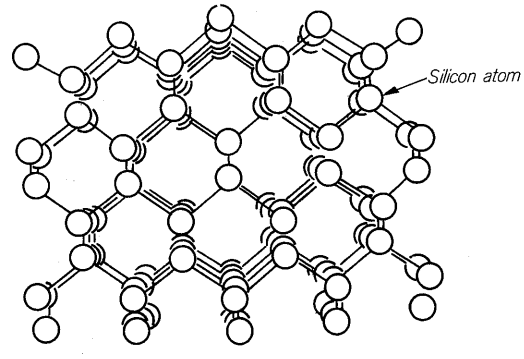

(a) Single crystal silicon

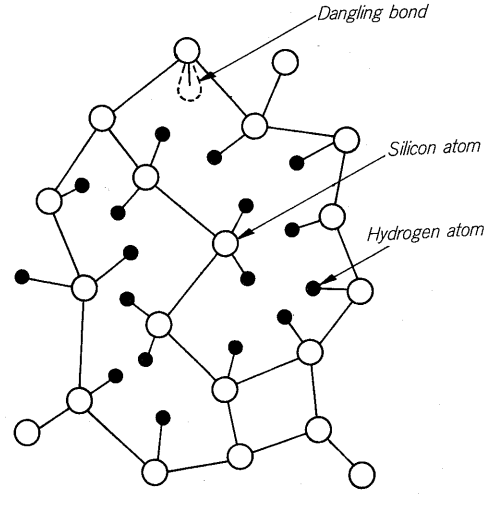

(b) Amorphous silicon

Fig. 1 Models of single crystal and amorphous silicon structures

solar cell is much less than that for the single crystal Si solar cell because of its low temperature growth (200 to 400°C); this contributes to reduce energy pay-back period.

(b) The optical absorption coefficient of the a-Si is greater than 10^4 cm^{-1} over the visible portion of the solar spectrum (*Fig. 2*) so that an efficient solar cell can be constructed by a thin film a-Si of about 1μm in thickness.

(c) A large area solar cell can be easily realized because the a-Si film is deposited by plasma decomposition of silane on an inexpensive substrate such as sheet metal or glass substrate.

(d) The fabrication processes of the a-Si solar cell are much simpler and have a greater potential to become automated in comparison with those of crystalline Si solar cells.

A key step to success for practical applications of the a-Si solar cell to photovoltaic power generation is to improve its cell performance. We have conducted a series of investigations on the a-Si material and its applications to solar cells. The results of these researches obtained up to the present time will be reported as follows.

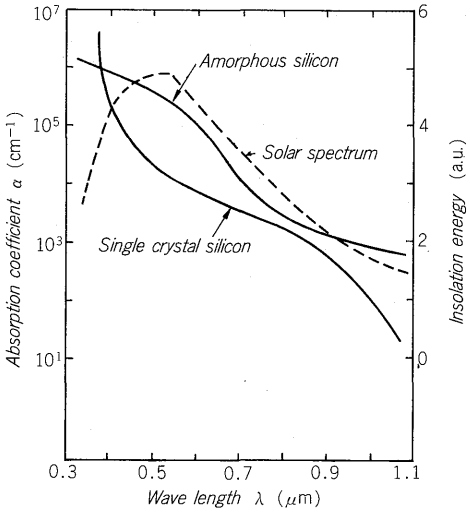

Fig. 2 Optical absorption spectra of a-Si.

III. THE a-Si FILM DEPOSITION TECHNIQUE

1. The a-Si film deposition condition

In 1975, Spear et al.[2] showed that the electronic properties of the hydrogenated amorphous silicon (a-Si:H) prepared by glow discharge decomposition of silane (SiH_4) could be controlled by a suitable impurity doping in the gas phase. In other words they showed that the thin film a-Si p-n junction could be realized by the glow discharge method.

Figure 3 shows a schematic diagram of the a-Si deposition system. SiH_4 gas is fed into the reactor, glow discharge is performed by DC or RF electric field, decomposed Si and

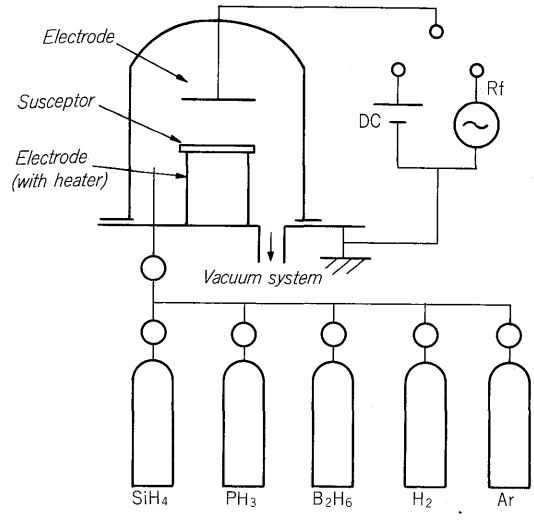

Fig. 3 Schematic diagram of a-Si deposition system

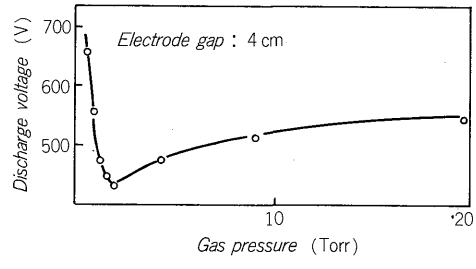

Fig. 4 Self-sustaining discharge voltage versus gas pressure

H are deposited on a substrate heated to 200°C-400°C, and thus the a-Si film is formed.

Properties of a-Si film considerably vary depending on the deposition condition and composition of deposition equipment. Therefore, relationships between deposition parameters and electronic and optoelectornic properties of the a-Si film in the glow discharge method were systematically examined. The result obtained by DC glow discharge is reported here as one of the examples[3]. Figure 4 shows a dependence of selfsustaining discharge voltage on pressure of 10% SiH_4 gas (diluted by hydrogen gas). In this case an electrode gap is fixed to 4 cm. The self-sustaining discharge voltage at first decreases abruptly with the gas pressure and increases gradually when the gas pressure becomes greater than 2 torr; this coincides with the well-known relation deduced from the Paschen's law.

Figures 5 and 6 indicate dependences of photoconductivity and growth rate of the a-Si film on deposition parameters (gas pressure in *Fig. 5* and discharge current in *Fig. 6*). The photocurrent denotes an electrical conductivity of the a-Si film when it is illuminated, and in a solar cell this value must be great. The photoconductivity was measured under AM2 illumination (equivalent to 75 mW/cm^2). As to the growth rate, the higher value is desirable from

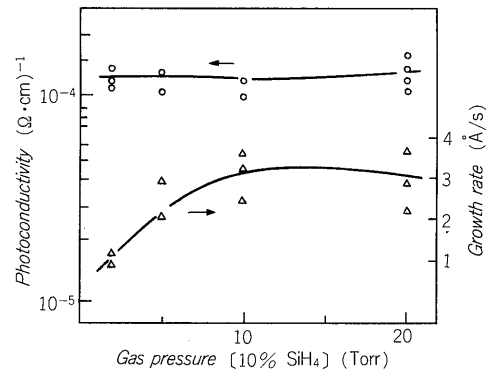

Fig. 5 Dependence of photoconductivity and growth rate on gas pressure

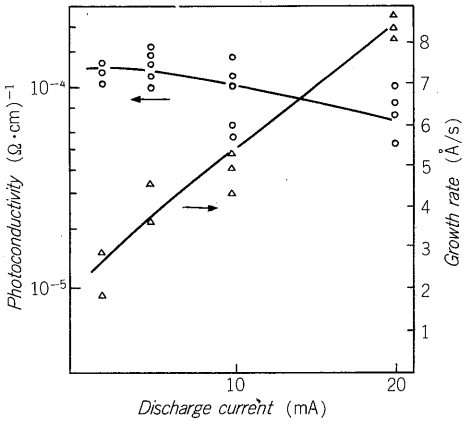

Fig. 6 Dependence of photoconductivity and growth rate on discharge current

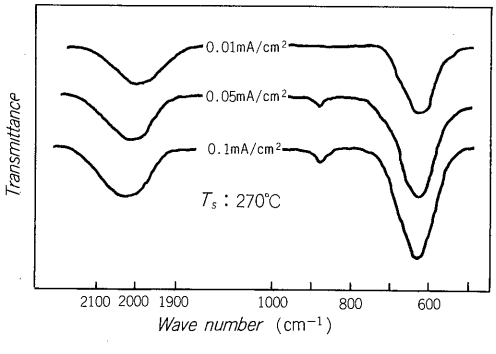

Fig. 7 Infrared transmission spectra of a-Si films and its dependence on discharge current for film growth

the practical view point. However, as it is obvious from *Fig. 6*, if the growth rate increase is intended by increasing discharge current, it will result in a reduction of the photoconductivity. The reduction of photoconductivity coincides with the appearance of absortion peak in the vicinity of 880 cm^{-1} in the infrared absorption spectra of the a-Si film shown in *Fig. 7*. The absorption peak is due to a vibration of Si-H_2 bonds [Refer to *Fig. 1* (b)], and the existence of this bond causes a degradation of photoconductive characteristics of the a-Si film. The absorption peaks observed at 630 cm^{-1} and 2000 cm^{-1} are due to the vibration of Si-H bond, and only these two absorptions appear in the infrared absorption spectra of a higher photoconductive a-Si film.

2. The doping of substitutional impurities to the a-Si film

An n-type a-Si and a p-type a-Si can be obtained respectively by introducing PH_3 and B_2H_6 gases into the reactor during the glow discharge of SiH_4 gas. Figure 8 shows the dependence of conductivity on temperature in the p-type and n-type a-Si films formed by a decomposition of gases with $B_2H_6/SiH_4 = 1.2\%$ and $PH_3/SiH_4 = 1.2\%$ respectively. In comparison with a nondoped (i-layer) a-Si to which no substitutional impurities are added, the electrical conductivity at room temperature increases by 3-4 orders of magnitude and the activation energy reduces at the same time.

Properties of the doped layer also depend on the deposition conditions. The deposition condition for the boron doped p-type layer in a pin type a-Si solar cell [*Fig. 10* (b)] must be controlled to minimize the light absorption in the p layer. Figure 9 shows an example of the relations between the characteristics of the p-type a-Si film and the deposition temperature[4]. As the deposition temperature rises, an activation energy (E_a) and an optical band gap (E_g opt) reduce, while the electrical conductivity (σ) increases.

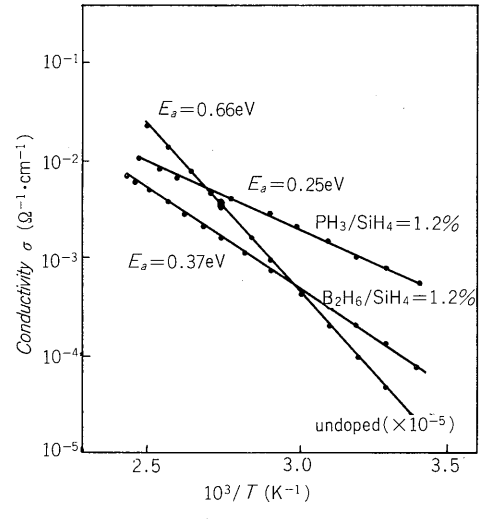

Fig. 8 Temperature dependence of conductivity of a-Si films

IV. THE a-Si SOLAR CELL

1. The structure of the a-Si solar cell

Figure 10 shows schematic structures of four types of large area a-Si solar cells being studied by Fuji Electric.

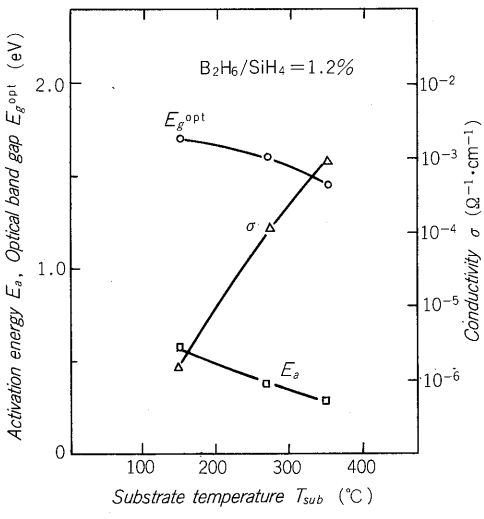

Fig. 9 p-type a-Si characteristics versus deposition temperature

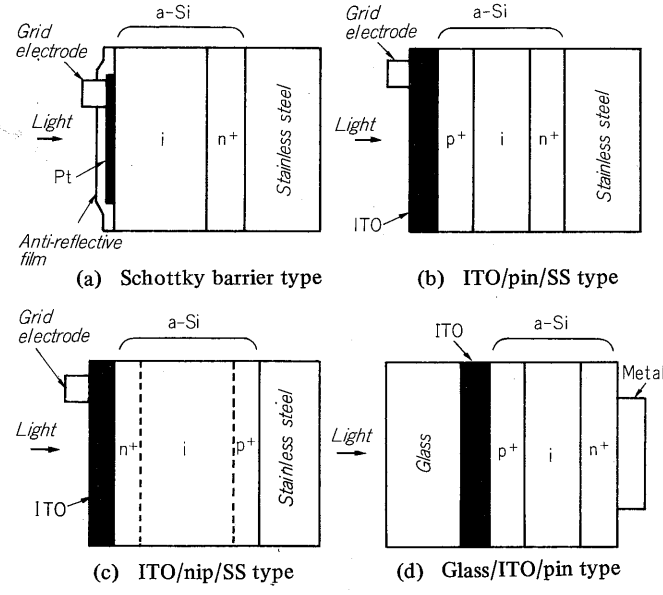

Fig. 10 Schematic structures of a-Si solar cells

Three types of solar cells shown in *Fig. 10* (a) through (c) use stainless steel substrates, and these solar cells are intended for photovoltaic power generation. When our research started four years ago, few studies on the large area solar cell had been reported. However, we confirmed that a uniform a-Si silm could be formed on substrates placed on a 200 cm^2 susceptor in the deposition apparatus which was originally designed by Fuji Electric. Then the work has been conducted mainly on 49 cm^2 solar cells whose area is suitable to practical use. In the early stage, the Schottky barrier type shown in *Fig. 10* (a) was studied. At present, however, our researching emphasis is placed on the pin and inverted pin types [*Fig. 10* (b) and (c)] because the junction can be completed simultaneously in the a-Si deposition process.

ITO (In_2O_3-SnO_2) is used for the transparent conductive film in the pin and inverted pin type cells. A refractive index of the ITO is about 2, and it is very convenient to use the ITO because it also functions as an antireflective film. Figure 11 shows a 100 cm^2 a-Si solar cell. For a large area a-Si solar cell, a grid electrode configutation must be optimized to get a large active cell area without output power lowering by series resistances in the transparent conductive film and grid electrodes.

The pin structure on the glass substrate shown in *Fig. 10* (d) has been examined for applications to such consumer electronics as electronic calculators, clocks and radios.

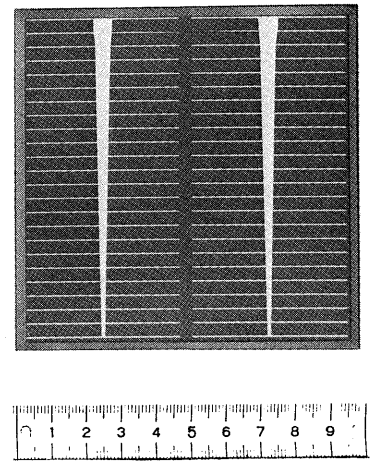

Fig. 11 10 cm x 10 cm a-Si solar cell

2. The characteristics of a-Si solar cells

When an a-Si solar cell is illuminated, electron and hole pairs are generated by an energy of the light. Then, the electron hole pairs are separated by an internal electric field in the junction, and collected toward electrodes, generating an electromotive force. Thus, an output current can be obtained through a load connected to the solar cell.

Figure 12 shows an energy band diagram of the pin type a-Si solar cell. Only the photocarriers generated in the region where the internal electric field exists (range indicated by W in *Fig. 12*) contributes to a photocurrent, because a carrier life time is short in the a-Si film obtained by the present deposition techique.

Figure 13 shows an output characteristics of the solar cell. The curve indicated as *Dark* represents dark forward J-V characteristics and the curve indicated as *Bright* represents output characteristics when the cell is illuminated. An actual solar cell output power is indicated by an shaded area in *Fig. 13*, and therefore, the conversion efficiency (η) is expressed as

$$\eta = \frac{I_m \times V_m}{\text{Energy incident on the solar cell}} \times 100\ (\%)$$

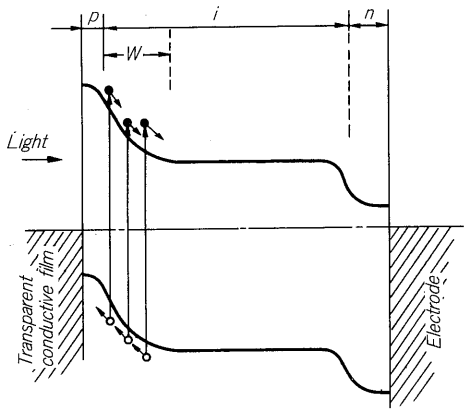

Fig. 12 Energy band diagram of pin type a-Si solar cell

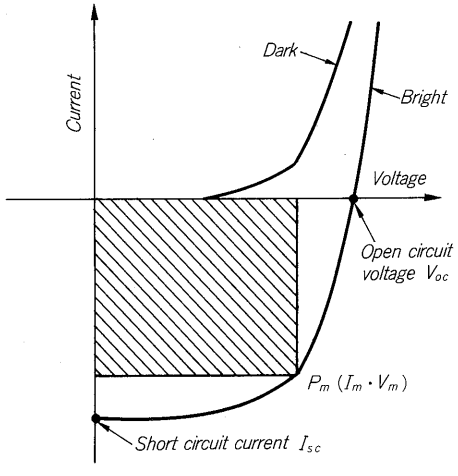

Fig. 13 Output characteristics of solar cell

The ratio of maximum output to (Short circuit current x Open circuit voltage), that is, $(I_m \cdot V_m)/(I_{sc} \cdot V_{oc})$ is defined as fill factor (FF).

Figure 14 shows the influence of the p-layer thickness of the pin type a-Si solar cell on the conversion efficiency, the short circuit current and the open circuit voltage. The sample has a 1.2 cm^2 pin type a-Si film formed on a stainless steel substrate together with Pt transparent conductive film and SiO antireflective film. The n-layer and i-layer thicknesses of the a-Si are respectively 350 Å and 5500 Å. The cell characteristics in *Fig. 14* were measured on the samples having different p-layer thicknesses in the junction structure. When the p-layer thickness is zero, the cell is a Pt Schottky barrier type solar cell. The values obtained from the Schottky barrier cell are also shown in *Fig. 14* to be compared with those of the pin cell.

A maximum efficiency of 4% was obtained for the pin type solar cell with about 70 Å p-layer thickness and this value is higher than that of the Schottky barrier type solar

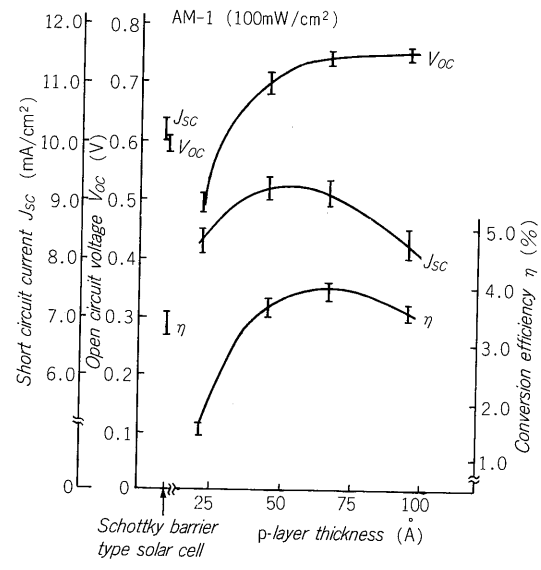

Fig. 14 Output characteristics and conversion efficiency versus p-layer thickness

cell. When the p-layer thickness is less than 30 Å, the open circuit voltage of the pin cell is lower than that of the Schottky cell, which may be caused by an incomplete formation of the pin junction.

The short circuit current increases as the p-layer thickness increases. It reaches the maximum when the p-layer thickness is about 50 Å, and reduces when the p-layer thickness exceeds 50 Å. It is assumed that the reduction of short circuit current is caused by an increase of light absorption in the p-layer and an increase of recombination of photocarriers.

The above mentioned SiO/Pt/pin/stainless steel cell was used only for the experiments. For power generation, solar cells of ITO/pin/stainless steel [*Fig. 10* (b)] or ITO/nip/stainless steel [*Fig. 10* (c)] are being developed. In the ITO/nip/stainless steel cell, maximum efficiencies of 6.47% (1.2 cm^2), 5.2% (49 cm^2) and 4.2% (100 cm^2) have been obtained so far[6]. Figure 15 shows output characteristics for the 6.47% maximum conversion efficiency and Figure 16 shows the relation of the conversion efficiency and solar cell areas[5],[6].

The inverted pin type cell has a higher efficiency than the pin type cell and also has a higher short circuit current, open circuit voltage and fill factor. The increase of short circuit current may be due to a greater transmittance of the n-layer a-Si than that of the p layer a-Si. The conversion efficiency tends to lower as the area of solar cell increases. This is mainly caused by a reduction of fill factor and an areal fluctuation of short circuit current[6]. The tasks to be accomplished next are to optimize junction and electrode structures of large area a-Si solar cells more precisely and to improve the conversion efficiency up to the value of a small area solar cell.

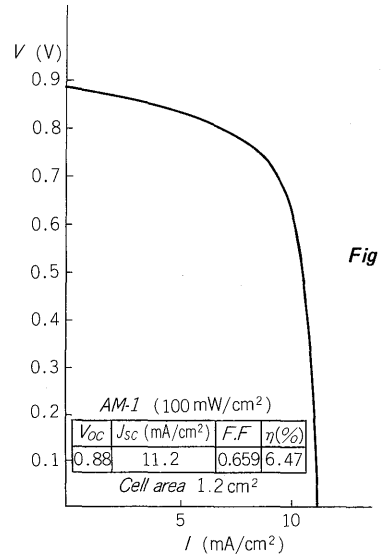

Fig 15. Output characteristics of a-Si solar cell with 6.47%

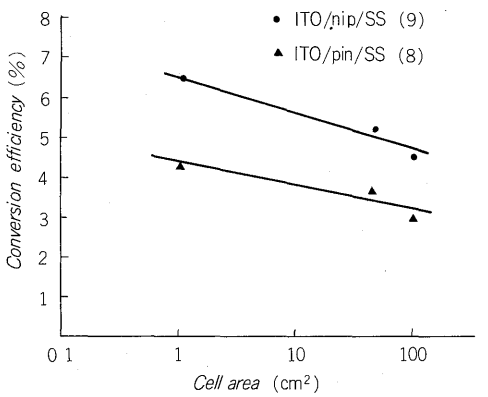

Fig. 16 Cell area dependence of conversion efficiency of a-Si solar cell

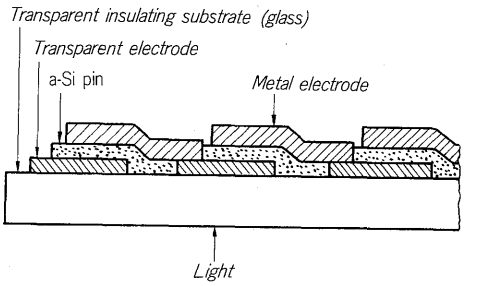

Fig. 17 Cascade type a-Si solar cell

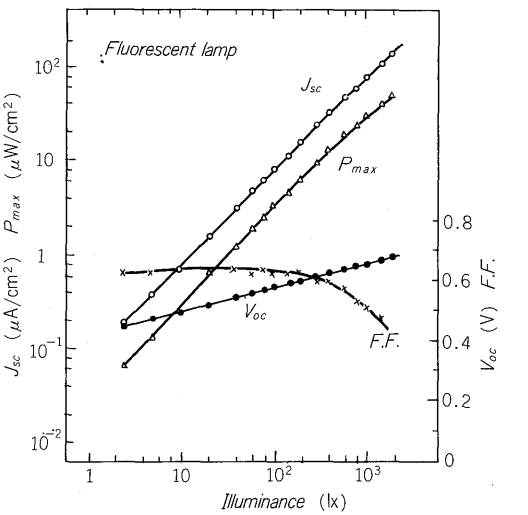

Fig. 18 Photovoltaic characteristics under fluorescent lamp

V. THE APPLICATIONS OF THE a-Si SOLAR CELL

The a-Si solar cell is applied to cosumer electronics as an power source of an electronic calculator, clock and watch. In case of a clock or a watch, it is used together with such a power source as a silver oxide battery to extend a service life of the battery. When a single crystal silicon cell is used for such applications, several cells must be connected in series on the small area circuit board through the wiring process in order to provide the device driving voltage (1.5 to 3.0 V). On the other hand, the a-Si solar cell can be connected in series without wiring. Figure 17 shows how to connect a-Si solar cells in series. Transparent electrodes are split-formed in advance on a piece of glass, and the a-Si of pin structure is formed on them. Then, metal electrodes are formed in such a pattern that a part of the metal electrode is overlapped with the tranparent electrode of the next cell. Therefore, cells can be connected in series simultaneously.

When solar cells are used as power sources of consumer electronics. the power generating ability under room light must be examined. Figure 18 shows one example of relationships between an illuminance under a fluorecent lamp and various characteristics of the a-Si solar cell. As we know from this figure, 0.6 V of the open circuit voltage, 16μA/cm^2 of the short circuit current and 6 μW/cm^2 of the output under the optimum load conditions were obtained under 200 lux. The output electric power is equal to or larger than that of a single crystal silicon solar cell under fluorescent lamp, and it can be explained from the similarity of wave length dependences of collection effciency of a-Si and fluorescent lamp radiation spectra as shown in *Fig. 19*. It shows the collection efficiency measured by a constant energy spectrometer under an incident light of 150μW/cm^2. The a-Si solar cell for a electronic calculator has already been put on the market. It is believed that the a-Si solar cells will be used for various other applications in the near future. Figure 20 shows a-Si solar cells for electronic calculator, and *Table 1* lists characteristics of the a-Si solar cells presently on the market.

Figure 21 shows an a-Si solar cell module which consists of 36 sheets of 49 cm^2 solar cells made by Fuji Electric.

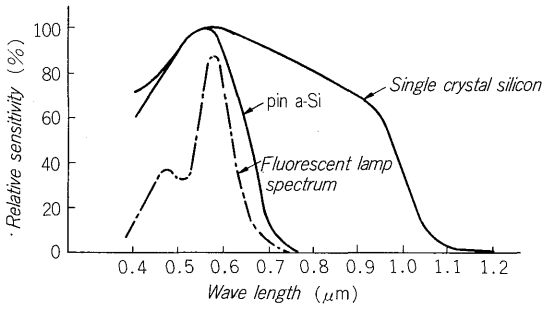

Fig. 19 Collection efficiency

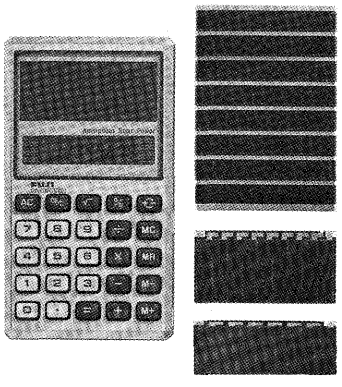

Fig. 20 a-Si solar cells for consumer use

Table 1 Characteristics of a-Si solar cells for consumer electronics

Model	ELA001	ELA003	ELA011	ELA012	ELA021
Size (mm)	55 x 8	27 x 55	13.5 x 55	18.3 x 40.5	55 x 81
Area	3cm² x 10	1.18cm² x9	0.97cm² x5	1cm² x5	4cm² x8
Maximum output	90μW	30μW	15μW		48mW
Voltage	3 V	3 V	1.5 V		3 V
current	30μA	10μA	10μA		16mA
Condition	Fluorescent lamp (200 lux)				Sun light (50mW/cm²)

Figure 22 shows a solar cell array which consists of 108 pieces of this module. This solar cell array has an about 400 W power generating ability under AM1. It was installed as a joint work between The Tokyo Electric Power Co., Inc. and Fuji Electric in the spring of 1981, and is now under field test to evaluate the system reliability.

VI. SUMMARY

In this paper, we presented the recent progress in a-Si solar cell researches conducted by Fuji Electric. A remarkable progress has been obtained in cell performances of large area a-Si:H solar cells on stainless steel substrates.

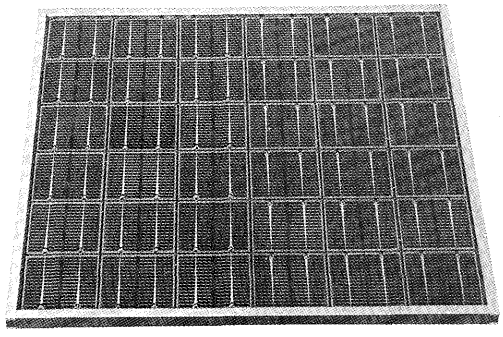

Fig. 21 a-Si solar cell module

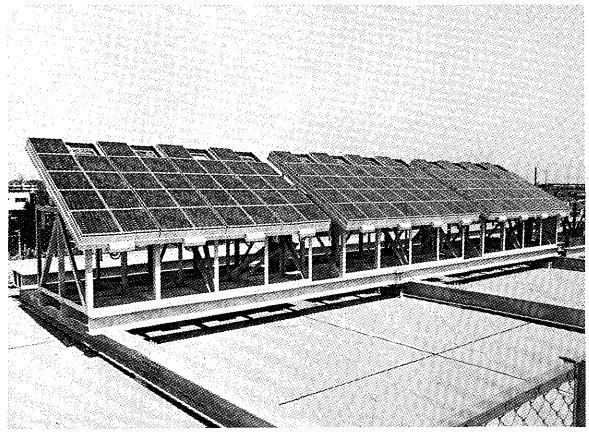

Fig. 22 a-Si solar cell array (400W under AM1)

In the field of the application to consumer electronics, Fuji Electric has developed a series of fluorescent sensitive photovoltaic cells having glass substrates, which have been supplied to several pocket calculator manufacturers since mid-1980.

The conversion efficiency improvement of the a-Si solar cells might be directly connected to the cost reduction of the photovoltaic system. From this point of view, a wide range of researches in both material science and application field are under way in Fuji Electric.

VII. ACKNOWLEDGEMENT

The authors are grateful to Prof. Y. Hamakawa of Osaka Univercity for his helpful discussions.

This work was partly supported by the Agency of Industrial Science and Technology as Sunshine Project.

References:

(1) J.C. Knights: Jpn. J. Appl. Phys., 18, Supplement 18-1 (1979).
(2) W.E. Spear and P.G. LeComber: Solid State Commun., 17 (1975).
(3) T. Ichimura et al.: Extended Abstracts of 158th Electrochemical Society Meeting, Florida, Vol. 80-2 (1980).
(4) Y. Uchida et al.: Proc. 8th International Vacuum Congress, Cannes, Vol. 1 (1980).
(5) Y. Uchida et al.: Proc. 2nd Photovoltaic Sci. and Eng. Conf. in Japan, Tokyo (1980) and Jpn. J. Appl. Phys., 2 (1980).
(6) Y. Uchida et al.: Proc. IEEE 15th Photovoltaic Specialists Conf., Florida (1981).